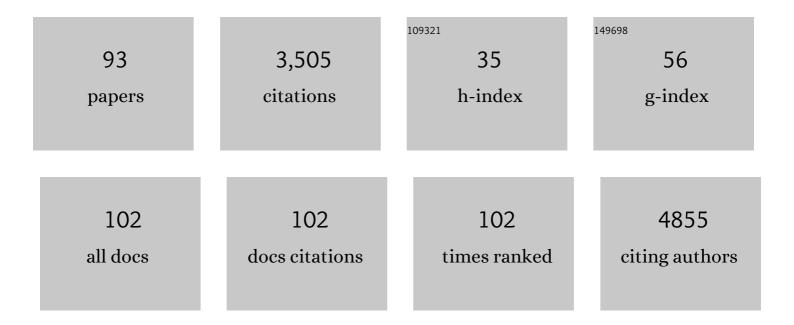
List of Publications by Year in descending order

Source: https://exaly.com/author-pdf/7673721/publications.pdf Version: 2024-02-01



Ιμῶς Μ Μλερλ

#	Article	IF	CITATIONS
1	Characterization of an extracellular polysaccharide produced by a Pseudomonas strain grown on glycerol. Bioresource Technology, 2009, 100, 859-865.	9.6	186
2	Adsorption and Activation of CO <sub>2</sub> by Amine-Modified Nanoporous Materials Studied by Solid-State NMR and <sup>13</sup> CO <sub>2</sub> Adsorption. Chemistry of Materials, 2011, 23, 1387-1395.	6.7	175
3	Interconvertable Modular Framework and Layered Lanthanide(III)-Etidronic Acid Coordination Polymers. Journal of the American Chemical Society, 2008, 130, 150-167.	13.7	153
4	Packing Interactions in Hydrated and Anhydrous Forms of the Antibiotic Ciprofloxacin: a Solid-State NMR, X-ray Diffraction, and Computer Simulation Study. Journal of the American Chemical Society, 2012, 134, 71-74.	13.7	128
5	Structure of Chemisorbed CO <sub>2</sub> Species in Amine-Functionalized Mesoporous Silicas Studied by Solid-State NMR and Computer Modeling. Journal of the American Chemical Society, 2017, 139, 389-408.	13.7	107
6	Water‣oluble Polymeric Carbon Nitride Colloidal Nanoparticles for Highly Selective Quasiâ€Homogeneous Photocatalysis. Angewandte Chemie - International Edition, 2020, 59, 487-495.	13.8	107
7	Solid acids with SO <sub>3</sub> H groups and tunable surface properties: versatile catalysts for biomass conversion. Journal of Materials Chemistry A, 2014, 2, 11813-11824.	10.3	98
8	Multi-functional rare-earth hybrid layered networks: photoluminescence and catalysis studies. Journal of Materials Chemistry, 2009, 19, 2618.	6.7	90
9	Sulfonated Graphene Oxide as Effective Catalyst for Conversion of 5â€(Hydroxymethyl)â€2â€furfural into Biofuels. ChemSusChem, 2014, 7, 804-812.	6.8	90
10	Synthesis of an O-alkynyl-chitosan and its chemoselective conjugation with a PEG-like amino-azide through click chemistry. Carbohydrate Polymers, 2012, 87, 240-249.	10.2	83
11	Amine functionalized porous silica for CO2/CH4 separation by adsorption: Which amine and why. Chemical Engineering Journal, 2018, 336, 612-621.	12.7	75
12	Energy Transfer and Emission Quantum Yields of Organicâ^'Inorganic Hybrids Lacking Metal Activator Centers. Journal of Physical Chemistry C, 2007, 111, 3275-3284.	3.1	70
13	Photoluminescent Lanthanideâ^'Organic 2D Networks:  A Combined Synchrotron Powder X-ray Diffraction and Solid-State NMR Study. Chemistry of Materials, 2007, 19, 3527-3538.	6.7	67
14	A Simple Mechanochemical Route to Layered Double Hydroxides: Synthesis of Hydrotalciteâ€Like Mgâ€Alâ€NO <sub>3</sub> â€LDH by Manual Grinding in a Mortar. Zeitschrift Fur Anorganische Und Allgemeine Chemie, 2009, 635, 1470-1475.	1.2	66
15	Series of Metal Organic Frameworks Assembled from Ln(III), Na(I), and Chiral Flexible-Achiral Rigid Dicarboxylates Exhibiting Tunable UV–vis–IR Light Emission. Inorganic Chemistry, 2012, 51, 1703-1716.	4.0	63
16	High-resolution 1H homonuclear dipolar recoupling NMR spectra of biological solids at MAS rates up to 67kHz. Journal of Magnetic Resonance, 2009, 199, 111-114.	2.1	62
17	Catalytic dehydration of fructose to HMF over sulfonic acid functionalized periodic mesoporous organosilicas: role of the acid density. Catalysis Science and Technology, 2014, 4, 2235-2240.	4.1	62
18	Mesoporous carbon–silica solid acid catalysts for producing useful bio-products within the sugar-platform of biorefineries. Green Chemistry, 2014, 16, 4292-4305.	9.0	62

#	Article	IF	CITATIONS
19	Clean synthesis of molecular recognition polymeric materials with chiral sensing capability using supercritical fluid technology. Application as HPLC stationary phases. Biosensors and Bioelectronics, 2010, 25, 1742-1747.	10.1	59
20	Layered double hydroxides with interlayer borate anions: A critical evaluation of synthesis methodology and pH-independent orientations in nano-galleries. Applied Clay Science, 2011, 51, 308-316.	5.2	58
21	X-ray and NMR Crystallography Studies of Novel Theophylline Cocrystals Prepared by Liquid Assisted Grinding. Crystal Growth and Design, 2015, 15, 3674-3683.	3.0	57
22	Chitin–glucan complex production by Komagataella pastoris : Downstream optimization and product characterization. Carbohydrate Polymers, 2015, 130, 455-464.	10.2	55
23	KCa4(BO3)3:Ln3+ (Ln = Dy, Eu, Tb) phosphors for near UV excited white–light–emitting diodes. AlP Advances, 2013, 3, .	1.3	53
24	Rationalizing the role of the anion in CO <sub>2</sub> capture and conversion using imidazolium-based ionic liquid modified mesoporous silica. RSC Advances, 2015, 5, 64220-64227.	3.6	53
25	Practical aspects of Lee–Goldburg based CRAMPS techniques for high-resolution 1H NMR spectroscopy in solids: Implementation and applications. Journal of Magnetic Resonance, 2008, 194, 264-282.	2.1	51
26	A supramolecular strategy based on molecular dipole moments for high-quality covalent organic frameworks. Chemical Communications, 2016, 52, 7986-7989.	4.1	50
27	Multinuclear solid-state NMR characterization of the BrÃ,nsted/Lewis acid properties in the BP HAMS-1B (H-[B]-ZSM-5) borosilicate molecular sieve using adsorbed TMPO and TBPO probe molecules. Journal of Catalysis, 2014, 316, 240-250.	6.2	46
28	NMR Crystallography: Toward Chemical Shift-Driven Crystal Structure Determination of the β-Lactam Antibiotic Amoxicillin Trihydrate. Crystal Growth and Design, 2013, 13, 2390-2395.	3.0	45
29	Optimised hydrothermal synthesis of multi-dimensional hybrid coordination polymers containing flexible organic ligands. Progress in Solid State Chemistry, 2005, 33, 113-125.	7.2	44
30	Structural Characterization of Zeolites by Advanced Solid State NMR Spectroscopic Methods. Annual Reports on NMR Spectroscopy, 2012, 77, 259-351.	1.5	44
31	Interaction of CO <sub>2</sub> and CH <sub>4</sub> with Functionalized Periodic Mesoporous Phenylene–Silica: Periodic DFT Calculations and Gas Adsorption Measurements. Journal of Physical Chemistry C, 2016, 120, 3863-3875.	3.1	41
32	Combining Multinuclear High-Resolution Solid-State MAS NMR and Computational Methods for Resonance Assignment of Glutathione Tripeptide. Journal of Physical Chemistry A, 2012, 116, 6711-6719.	2.5	40
33	Production of yeast chitin–glucan complex from biodiesel industry byproduct. Process Biochemistry, 2012, 47, 1670-1675.	3.7	39
34	Identifying Selective Host–Guest Interactions Based on Hydrogen Bond Donor–Acceptor Pattern in Functionalized Al-MIL-53 Metal–Organic Frameworks. Journal of Physical Chemistry C, 2013, 117, 19991-20001.	3.1	38
35	Chirality-Dependent Growth of Self-Assembled Diphenylalanine Microtubes. Crystal Growth and Design, 2019, 19, 6414-6421.	3.0	38
36	Photoluminescent Rare-Earth Based Biphenolate Lamellar Nanostructures. Journal of Physical Chemistry C, 2007, 111, 2539-2544.	3.1	37

#	Article	IF	CITATIONS
37	Carboxylate-intercalated layered double hydroxides aged under microwave–hydrothermal treatment. Journal of Solid State Chemistry, 2009, 182, 18-26.	2.9	36
38	Unravelling the Structure of Chemisorbed CO <sub>2</sub> Species in Mesoporous Aminosilicas: A Critical Survey. Environmental Science & Technology, 2019, 53, 2758-2767.	10.0	36
39	Hydrothermal synthesis, crystal structures and photoluminescence properties of mixed europium–yttrium organic frameworks. Journal of Solid State Chemistry, 2012, 186, 165-170.	2.9	35
40	Metal Organic Frameworks Assembled from Y(III), Na(I), and Chiral Flexible-Achiral Rigid Dicarboxylates. Inorganic Chemistry, 2010, 49, 7917-7926.	4.0	34
41	Understanding the high catalytic activity of propylsulfonic acid-functionalized periodic mesoporous benzenesilicas by high-resolution 1H solid-state NMR spectroscopy. Journal of Materials Chemistry, 2012, 22, 7412.	6.7	31
42	Thermal and mechanical stability of lanthanide-containing glass–ceramic sealants for solid oxide fuel cells. Journal of Materials Chemistry A, 2014, 2, 1834-1846.	10.3	31
43	Packing Interactions and Physicochemical Properties of Novel Multicomponent Crystal Forms of the Anti-Inflammatory Azelaic Acid Studied by X-ray and Solid-State NMR. Crystal Growth and Design, 2016, 16, 154-166.	3.0	30
44	A general nonaqueous route to crystalline alkaline earth aluminate nanostructures. Nanoscale, 2009, 1, 360.	5.6	29
45	Diazole-based powdered cocrystal featuring a helical hydrogen-bonded network: Structure determination from PXRD, solid-state NMR and computer modeling. Solid State Nuclear Magnetic Resonance, 2015, 65, 49-63.	2.3	28
46	Unravelling moisture-induced CO <sub>2</sub> chemisorption mechanisms in amine-modified sorbents at the molecular scale. Journal of Materials Chemistry A, 2021, 9, 5542-5555.	10.3	28
47	Multiplex MQMAS NMR of quadrupolar nuclei. Solid State Nuclear Magnetic Resonance, 2005, 28, 13-21.	2.3	27
48	Characterization of Layered Î <sup>3</sup> -Titanium Phosphate (C2H5NH3)[Ti(H1.5PO4)(PO4)]2·H2O Intercalate: A Combined NMR, Synchrotron XRD, and DFT Calculations Study. Chemistry of Materials, 2008, 20, 3944-3953.	6.7	27
49	What Is Being Measured with P-Bearing NMR Probe Molecules Adsorbed on Zeolites?. Journal of the American Chemical Society, 2021, 143, 13616-13623.	13.7	27
50	Structural Characterization of Layered Î <sup>3</sup> -Titanium Phosphate (C6H13NH3)[Ti(HPO4)(PO4)]·H2O. Chemistry of Materials, 2005, 17, 6287-6294.	6.7	24
51	Strategies for copper bis(oxazoline) immobilization onto porous silica based materials. Microporous and Mesoporous Materials, 2012, 158, 26-38.	4.4	24
52	1H–31P HETCOR NMR elucidates the nature of acid sites in zeolite HZSM-5 probed with trimethylphosphine oxide. Chemical Communications, 2019, 55, 12635-12638.	4.1	23
53	Hydrothermal synthesis, structural characterisation and magnetic behaviour of hybrid complexes of N-(phosphonomethyl)iminodiacetate. Journal of Molecular Structure, 2005, 754, 51-60.	3.6	21
54	Detecting Proton Transfer in CO <sub>2</sub> Species Chemisorbed on Amineâ€Modified Mesoporous Silicas by Using <sup>13</sup> Câ€NMR Chemical Shift Anisotropy and Smart Control of Amine Surface Density. Chemistry - A European Journal, 2018, 24, 10136-10145.	3.3	21

#	Article	IF	CITATIONS
55	2D Layered Dipeptide Crystals for Piezoelectric Applications. Advanced Functional Materials, 2021, 31, 2102524.	14.9	21
56	Boron removal and reinsertion studies in 10 B– 11 B exchanged HAMS-1B (H-[B]-ZSM-5) borosilicate molecular sieves using solid-state NMR. Journal of Catalysis, 2016, 334, 14-22.	6.2	20
57	New Crystalline Layered Zinc Phosphate with 10-Membered-Ring Channels Perpendicular to Layers. Inorganic Chemistry, 2009, 48, 4598-4600.	4.0	19
58	Understanding Polymorphic Control of Pharmaceuticals Using Imidazolium-Based Ionic Liquid Mixtures as Crystallization Directing Agents. Crystal Growth and Design, 2017, 17, 428-432.	3.0	19
59	Enhancing Adamantylamine Solubility through Salt Formation: Novel Products Studied by X-ray Diffraction and Solid-State NMR. Crystal Growth and Design, 2019, 19, 1860-1873.	3.0	19
60	1H–1H double-quantum CRAMPS NMR at very-fast MAS (μ2R=35kHz): A resolution enhancement method to probe 1H–1H proximities in solids. Journal of Magnetic Resonance, 2009, 196, 88-91.	2.1	18
61	Assessing the performance of windowed 1H CRAMPS methods, on biological solids, at high-field and MAS up to 35kHz. Journal of Magnetic Resonance, 2009, 197, 20-27.	2.1	18
62	Combining STMAS and CRAMPS NMR spectroscopy: High-resolution HETCOR NMR spectra of quadrupolar and 1H nuclei in solids. Chemical Physics Letters, 2009, 470, 337-341.	2.6	18
63	Co <sup>II</sup> /Zn <sup>II</sup> –( <scp>L</scp> ‶yrosine) Magnetic Metal–Organic Frameworks. European Journal of Inorganic Chemistry, 2012, 2012, 5259-5268.	2.0	18
64	X-ray Diffraction and Solid-State NMR Studies of a Germanium Binuclear Complex. Chemistry - A European Journal, 2006, 12, 363-375.	3.3	17
65	Revisiting the Thermal Decomposition of Layered γ-Titanium Phosphate and Structural Elucidation of Its Intermediate Phases. Inorganic Chemistry, 2010, 49, 2630-2638.	4.0	17
66	Waterâ€ <del>S</del> oluble Polymeric Carbon Nitride Colloidal Nanoparticles for Highly Selective Quasiâ€Homogeneous Photocatalysis. Angewandte Chemie, 2020, 132, 495-503.	2.0	15
67	Characterization of microporous aluminophosphate IST-1 using 1H Lee–Goldburg techniques. Journal of Magnetic Resonance, 2006, 180, 236-244.	2.1	14
68	Crystal Structure, Solid-State NMR Spectroscopic and Photoluminescence Studies of Organic-Inorganic Hybrid Materials (HL)6[Ge6(OH)6(hedp)6]·2(L)·nH2O, L = hqn or phen. European Journal of Inorganic Chemistry, 2006, 2006, 4741-4751.	2.0	14
69	Two novel supramolecular organic–inorganic adducts containing dibenzo-30-crown-10 and H3PM12O40 (M=W or Mo). Journal of Molecular Structure, 2008, 888, 99-106.	3.6	14
70	3D–2D–0D Stepwise Deconstruction of a Water Framework Templated by a Nanoporous Organic–Inorganic Hybrid Host. Chemistry - A European Journal, 2010, 16, 7741-7749.	3.3	14
71	Microwave assisted N-alkylation of amine functionalized crystal-like mesoporous phenylene-silica. Dalton Transactions, 2013, 42, 5631.	3.3	14
72	Melilite glass–ceramic sealants for solid oxide fuel cells: effects of ZrO2 additions assessed by microscopy, diffraction and solid-state NMR. Journal of Materials Chemistry A, 2013, 1, 6471.	10.3	13

#	Article	IF	CITATIONS
73	Yttrium-succinates coordination polymers: Hydrothermal synthesis, crystal structure and thermal decomposition. Journal of Solid State Chemistry, 2009, 182, 3365-3373.	2.9	12
74	Microwave-assisted N,N-dialkylation of amine-functionalized periodic mesoporous phenylene-silica: An easy and fast way to design materials. Microporous and Mesoporous Materials, 2017, 249, 10-15.	4.4	11
75	A pentanuclear oxovanadium(V) phosphate complex with phenanthroline. Inorganic Chemistry Communication, 2006, 9, 34-38.	3.9	10
76	"Hidden―CO <sub>2</sub> in Amine-Modified Porous Silicas Enables Full Quantitative NMR Identification of Physi- and Chemisorbed CO <sub>2</sub> Species. Journal of Physical Chemistry C, 2021, 125, 14797-14806.	3.1	10
77	Storage and delivery of H2S by microporous and mesoporous materials. Microporous and Mesoporous Materials, 2021, 320, 111093.	4.4	8
78	Moisture effect on the separation of CO2/CH4 mixtures with amine-functionalised porous silicas. Chemical Engineering Journal, 2022, 443, 136271.	12.7	8
79	Synthetic and Catalytic Potential of Amorphous Mesoporous Aluminosilicates Prepared by Postsynthetic Aluminations of Silica in Aqueous Media. ChemCatChem, 2018, 10, 1385-1397.	3.7	7
80	[Co(H2O)6]{[Co(C4H4N2)(H2O)2][V2O2(pmida)2]}·2H2O [H4pmida isN-(phosphonomethyl)iminodiacetic acid]: the first two-dimensional hybrid framework containing [V2O2(pmida)2]4â^'building blocks. Acta Crystallographica Section E: Structure Reports Online, 2005, 61, m1628-m1632.	0.2	5
81	Revisiting the crystal structure of dickite: X-ray diffraction, solid-state NMR, and DFT calculations study. American Mineralogist, 2018, 103, 812-818.	1.9	4
82	Nature of the multicomponent crystal of salicylic acid and 1,2-phenylenediamine. CrystEngComm, 2020, 22, 708-719.	2.6	4
83	Quantification of BrÃ,nsted Acid Sites in Zeolites by Water Desorption Thermogravimetry. European Journal of Inorganic Chemistry, 2020, 2020, 1860-1866.	2.0	3
84	Elucidating the Germanium Distribution in ITQâ€13 Zeolites by Density Functional Theory**. Chemistry - A European Journal, 2022, 28, .	3.3	3
85	Hydrogen bonding networks in gabapentin protic pharmaceutical salts: NMR and in silico studies. Magnetic Resonance in Chemistry, 2019, 57, 243-255.	1.9	2
86	2D Layered Dipeptide Crystals for Piezoelectric Applications (Adv. Funct. Mater. 43/2021). Advanced Functional Materials, 2021, 31, 2170320.	14.9	2
87	Through-space hopping transport in an iodine-doped perylene-based metal–organic framework. Molecular Systems Design and Engineering, 2022, 7, 1065-1072.	3.4	2
88	Improving the 1H indirect dimension resolution of 2D CRAMPS NMR spectra: A simulation and experimental investigation. Solid State Nuclear Magnetic Resonance, 2011, 39, 81-87.	2.3	1
89	Combination of solid-state NMR, DFT and XRPD for determination of a theophylline:4-aminobenzoic acid cocrystal phase. Acta Crystallographica Section A: Foundations and Advances, 2015, 71, s491-s491.	0.1	0
90	Understanding packing interactions and physicochemical properties of novel multicomponent crystal forms of azelaic acid-based anti-inflamatory drugs combining X-ray and NMR. Acta Crystallographica Section A: Foundations and Advances, 2015, 71, s256-s257.	0.1	0

#	Article	IF	CITATIONS
91	CanÂionic liquids be the key forÂpharmaceutical polymorphic control?ÂGabapentin as a case study. Acta Crystallographica Section A: Foundations and Advances, 2016, 72, s360-s360.	0.1	Ο
92	Structural characterization of two novel chiral Y(III)-MOFs. Acta Crystallographica Section A: Foundations and Advances, 2009, 65, s299-s299.	0.3	0
93	Novel chiral MOFs constructed by both mixed metals and dicarboxylate ligands. Acta Crystallographica Section A: Foundations and Advances, 2010, 66, s260-s260.	0.3	Ο